Vibration Characteristics of Multi-Wall Carbon Nanotubes (MWCNT) Reinforced 3D-Fiber Metal Laminates (3D-FML)

B Soltannia[1*], P Mertiny[1], and F Taheri[2]
[1] Department of Mechanical Engineering, University of Alberta, Edmonton, AB, Canada
[2] Department of Mechanical Engineering, Dalhousie University, Halifax, NS, Canada
* Corresponding author (babak.soltannia@ualberta.ca)

ABSTRACT

Uncontrolled vibration in mechanical systems results in undesirable noise and may cause the eventual mechanical failure of the system. This paper explores the parameters that govern and affect the frequency response of a novel 3D-fiber metal laminate (3D-FML). Specifically, the frequency response of the 3D-FML is evaluated and its vibration response is enhanced by an effective solution. The results obtained by the various approaches are presented and compared to the results obtained by a traditional approach. Moreover, the damping of the system could be enhanced quite significantly, up to 3.49 times, when only 1 wt% multi-wall carbon nanotubes was used to reinforce the system.

KEYWORDS: *vibration; damping; non-destructive testing; fiber-metal laminate; laser Doppler vibrometer*

1 INTRODUCTION

Fiber-reinforced polymer (FRP) composites are widely used in various structural applications in the aerospace, infrastructure, marine, automotive, offshore/onshore oil and gas industries, due to their superior strength- and stiffness-to-weight ratios and durability, to mention a few, all of which make them more effective compared to other materials (Berthelot, 1999; Reddy, 2004; Hyer, 2009). Amongst their other positive attributes is their vibration damping characteristics. This property is an important feature of this class of materials, since unwanted and unharnessed vibration in structures results in undesirable noise and potential mechanical failure. Such problems are often encountered in transport vehicles' body components, airplane cabins, and train and subway enclosures.

Several theoretical, numerical and experimental studies have considered vibration analyses of laminate or sandwich composite materials and structures (Sayyad and Ghugal, 2015). In 1973, Noor (1973) pointed out the inadequacies of the available analytical models for evaluation of low frequency vibration of thick simply-supported (SS) composite beams.

Improving the damping characteristics of laminated or sandwich composite plates has also been investigated experimentally by several researchers. The use of inherently damped materials and nanoparticles (NPs) as passive damping tools and harnessing of the external damping sources (as active damping technique) have been identified as effective techniques for enhancing the dynamic damping properties of composite materials and structures. The advantages of including small amounts of NPs to improve mechanical and electrical properties of resins used as the matrix in composite structures, as well as for adhesives, have also extensively been investigated by several researchers in the past (Ahmadi-Moghadam et al., 2013; Soltannia and Taheri, 2013 and 2014; Soltannia et al., 2013 and 2016; Taheri,

2017). Ahmadi-Moghadam et al. (2015) showed that using chemically functionalized Graphene Nanoplatelets (GNPs) had more influence on improving the mechanical properties of composite materials compared to non-functionalized GNPs. Liu et al. (2011) investigated the effect of functionalized single-wall carbon nanotubes (SWCNTs) on the damping properties of composite materials. DeValve and Pitchumani (2013) experimentally investigated the effect of inclusion of CNTs on damping enhancement of carbon fiber reinforced polymer (CFRP) laminated composite beams. They demonstrated that including 1-2 wt% CNTs could lead to 40-60% increase in the damping properties of CFRP composite beams. Khan et al. (2011) also showed that the inclusion of multi-wall carbon nanotubes (MWCNTs) slightly enhanced the damping properties of cantilever CFRP composite beams. They highlighted that the gain in properties came as a result of enhanced beam stiffness due to improved stiffness of the resin by the MWCNTs. In another study, Lei et al. (2015) used the Ritz method to investigate the damping properties of functionally graded (FG) CNTs reinforced thin laminate composite plates with clamped boundary conditions.

Zou et al. (2003), and De Cicco and Taheri (2018b) experimentally investigated the vibration characteristics of laminated and sandwich composite beams using non-destructive testing (NDT) techniques, similar to the investigation conducted by Cheraghi et al. (2007), who used the impulse excitation technique to establish material damping characteristics of polyvinyl chloride (PVC) pipes by using piezoelectric sensors to record the vibration response. Hajikhani et al. (2009) used an acoustic emission (AE) NDT technique to determine the presence and extent of defects.

Conventional 2D fiber-metal laminates (FMLs) have gained increasing application in the aerospace industry (Asundi and Choi, 1997). A new rendition of FMLs, in the form of a new class of three-dimensional FMLs (3D-FMLs) was recently introduced by Asaee and Taheri (2016). This new class of FMLs has superior static and dynamic strengths and offers excellent crashworthiness (De Cicco and Taheri, 2018a), thus has a great potential for use in applications in the automobile and aerospace industries. A 3D-FML is a sandwich composite consisting of a novel 3D fiberglass fabric with cavities through its thickness, sandwiched between sheets of lightweight metallic alloys (e.g., aluminum or magnesium).

As stated earlier, several studies have demonstrated the superior performance of this hybrid system under various loading conditions (Asaee and Taheri, 2016; De Cicco and Taheri, 2018a and 2018b). However, it is postulated that the dynamic response of the composite could be further improved by the inclusion of an optimal amount of a suitable nanoparticle filler. In this regard, an attempt is made to improve the damping characteristics of the material by the inclusion of NPs within the core and/or interface layers of the hybrid system. Moreover, it will be demonstrated that while the inclusion of MWCNT NPs improved the fundamental frequency of the system marginally, however, the damping of the system was enhanced quite significantly when only 1 wt% NP was used to reinforce the system.

2 MATERIALS AND METHODS

2.1 Materials

A three-dimensional fiberglass fabric (3DFGF) was obtained from China Beihai Fiberglass Co. (Jiujiang City, Jiangxi, China). Magnesium alloy sheets (AZ31B-H24; 0.5 mm thick) were acquired from MetalMart International (Commerce, CA, USA). Aluminium (6061-T6) was obtained from a local distributer. The hot-cure epoxy resin used to fabricate the 3DFGF and the core part of the 3D-FMLs composed of two parts (bisphenol-A-based Araldite LY 1564 resin and Aradur 2954 (cycloaliphatic polyamine) hardener) was purchased from Huntsman Co. (West Point, GA, USA). A two-part cold-cure thermoset epoxy resin (the West System 105 resin, and 206 hardener (Bay City, MI, USA)) was used for bonding the magnesium sheets to the core. The NP filler to be dispersed into the epoxy resin was MWCNTs with an outer diameter of 5 to 15 nm and more than 95% purity (obtained from the US Research Nanomaterials, Inc., Houston, TX, USA).

2.2 Specimen Preparation

3DFGF core sheets of 3D-FMLs were fabricated in situ using Huntsman hot-cure epoxy resin, by a hand brushing technique. Each panel was then cured in an oven at 60°C for two hours and at 120°C for

8 hours. At least three beam specimens with dimensions of 200 mm × 20 mm × 4 mm (length × width × thickness) were extracted out of each plate.

For the magnesium skins the bonding surfaces were roughened by grit-blasting, cleaned with an air gun, acetone washed and air-dried. The skins were then bonded to the core panels using the cold-cure epoxy resin and kept under vacuum for at least 24 hours at room temperature to assure optimal bonding. More details on the fabrication of 3D-FMLs can be found in Asaee and Taheri's work (2016).

For the NP dispersion, NPs were first distributed in the cold-cure resin system using a mechanical stirrer set at a speed of 2000 rpm for 10 minutes. Then, the NP resin slurry was calendered using a three-roll mill homogenizer (Torrey Hills Technologies LLC, San Diego, CA, USA). The roller gap was adjusted at 30 μm using a filler gauge for a 1 wt% (by weight) concentration of MWCNTs. In this study, the roller speed and calendering frequency were set constant at 174 rpm. To maximize the dispersion quality, calendering was conducted seven times. The curing agent was subsequently added to the slurry and mixed for 4–6 minutes using a stirrer set at a speed of 400 rpm. The mixture was then degassed under 28″ Hg vacuum for 2–3 minutes. Small specimens were extracted from different regions of the 3D-FGF cores using a jeweller saw. These specimens were placed on field emission scan electron microscopy (FESEM) stubs, and palladium-gold coated using the sputtering device (Leica Sputter Coating System Model ACE200, Wetzlar, Germany). FESEM was conducted using a Hitachi S-4700 field emission scanning electron microscope (Krefeld, Germany). Table 1 summarizes specimens' specifications.

Table 1 Specimen specification table

Specimen ID	Specimen specifications
Al	Aluminium alloy 6061-T6
3DFML1	0%Core-0%Interface-4mm 3DFML-Neat
3DFML6	0%Core-1%Interface-4mm 3DFML-MWCNT
3DFML7	1%Core-0%Interface-4mm 3DFML-MWCNT
3DFML8	1%Core-1%Interface-4mm 3DFML-MWCNT

2.3 Testing and analysis procedures

The experimental instruments used to acquire vibration signals are shown in Figure 1. Vibration data were recorded using a laser Doppler vibrometer (LDV) optical measurement system (LaserPoint LP01, OMS Co., Laguna Hills, CA, USA) as the non-contact method. Two pieces of prismatic low-density foam were used as supports to resemble free-free (F-F) boundary conditions (BCs). A light hammer, consisting of a steel ball as the stiff tip attached to a thin wooden rod (referred to as steel-wood hammer) was used to excite the specimens.

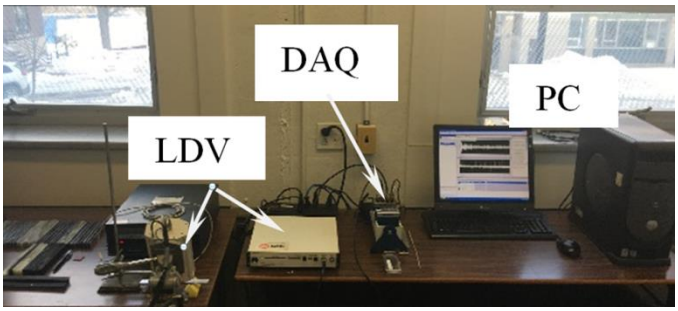

Figure 1: Experimental test setup for recording vibration signals of samples with free-free boundary conditions using the LDV

To be able to extract information regarding fundamental frequencies (f_1) and Damping Ratio (ζ), the entire oscillation spectrum ought to be captured. Hence, an LDV was connected to a data-acquisition

system, and the Signal Express software (National Instruments, Austin, TX, USA) was used to record the entire oscillation spectrum of each specimen at a 100 kHz sampling rate. The recorded information was then processed using LabVIEW (National Instruments). A reflective tape was used to increase the signal intensity.

2.4 Theoretical basis for evaluation of the vibration characteristics

2.4.1 Frequency and Damping Ratio

The fundamental frequencies obtained experimentally using the LDV were verified against those obtained by an available closed-form solution, extensively explained by several researchers (Berthelot, 1999 and 2005; Kelly, 1992; Tedesco *et al*., 1999; De Cicco and Taheri, 2018a), shown in equation (1):

$$f_n = \frac{1}{2\pi}\left(\frac{\gamma_n}{L}\right)^2 \sqrt{\frac{R}{\mu}} \quad with \quad R = \begin{cases} EI & \text{for homogenous beams} \\ bD_{11} & \text{for composite beams} \end{cases} \tag{1}$$

where, f_n is the natural frequency of n^{th} vibration mode (f_1 is the fundamental frequency), L is the length of the beam, R is the bending stiffness of the beam (EI for isotropic (homogeneous) beams, and bD_{11} for orthotropic (composite) beams), E is the modulus of elasticity, I is the moment of inertia of the cross-section, b is the width, D_{11} is the bending stiffness per unit width of the beam with respect to the longitudinal axis, μ is mass per unit length, and γ_n is the n^{th} solution of equation (2) (Tedesco, McDougal and Ross, 1999), obtained from solving the constitutive equation of motion for prismatic beams without any external loading and with F-F BCs, based on the stationary solution for deflection of a beam using the separation of variable technique (multiplication of time and displacement functions):

$$\cos\gamma \cosh\gamma = 1 \tag{2}$$

It has extensively been described by the aforementioned authors that the governing equation of a damped oscillatory motion can be mathematically represented by:

$$x_{(t)} = Ae^{-\xi\omega t}\cos(\omega_D t - \phi) \tag{3}$$

where, $x_{(t)}$ is the time-dependent equation of motion of a F-F damped vibrating system, A is the amplitude, with damping ratio $\xi < \xi_c = 1$, ξ_c is the critical damping ratio, ϕ is the phase angle, ω and ω_D are undamped and damped natural angular frequencies, respectively, which are related to one another through the following expression:

$$\omega_D = \omega\sqrt{1-\xi^2} \tag{4}$$

and

$$\omega = 2\pi f_n \tag{5}$$

It is worth mentioning that for damped vibration where $\xi < \xi_c = 1$, the amplitude is bound between two exponential curves called the signal envelope as it is shown in Figure 2(a).

The damping coefficient (ξ) can be determined through decremental logarithm (δ), over an oscillation period T_D, as the ratio of two adjacent amplitudes (consecutive maxima) of the i^{th} oscillation of the signal, represented mathematically as:

$$\xi = \frac{\delta_i}{\sqrt{4\pi^2 + \delta_i^2}} \quad (6)$$

To attain greater accuracy, the damping ratio could be evaluated over multiple oscillation periods instead of only one. Extractions of the decremental logarithm and damping coefficient were conducted using a LabVIEW code through exponential curve fitting and extraction of its power and coefficient.

2.4.2 Vibration signal extraction and analysis

As it was mentioned above, an LDV was used to obtain the natural frequency of the beam. The frequency obtained from the whole vibration signal spectrum and more particularly, the power spectrum, were computed using the Spectral Measurements subroutine of LabVIEW. This subroutine takes the vibration signal from the LDV and provides the amplitude of each frequency within the signal spectrum by performing Fast Fourier Transform (FFT) of the signal. Subsequently, the fundamental frequency is the frequency corresponding to the one with the largest amplitude, as shown in Figure 2(b).

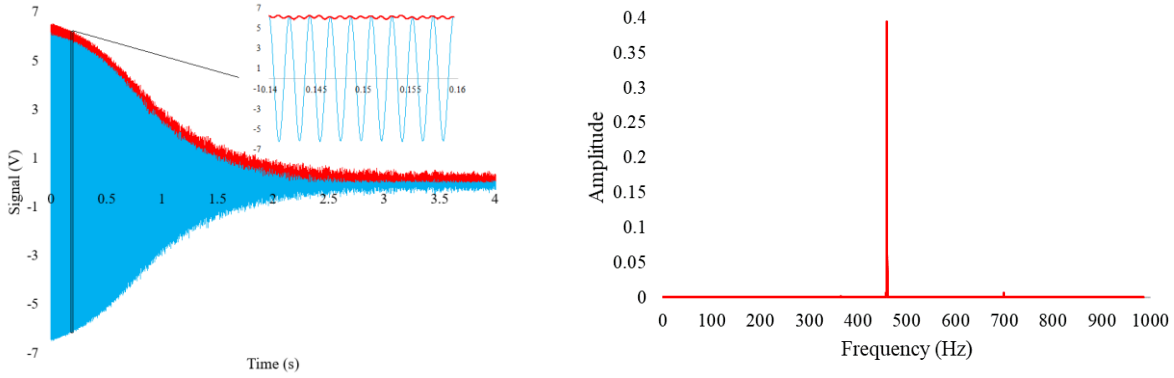

(a) (b)

Figure 2: Representation of (a) vibration signal and its representative envelope of Aluminum beam; (b) the power spectrum of aluminium beam

To calculate the damping coefficient, first, the signals were filtered in LabVIEW with a bandpass of ±30 Hz to mitigate noise. The envelope was then retrieved from the filtered signals using the Hilbert transform through the procedure described by Cheraghi et al. (2007), as schematically illustrated in Figure 2(a), using the following mathematical operation:

$$H(t) = \frac{1}{\pi}\int_{-\infty}^{+\infty} u(\tau)\frac{\chi(\tau)}{t-\tau}d\tau \quad (6)$$

In practice, if the envelope contains a complex number, its real part includes the signal's amplitude and its imaginary part contains the Hilbert operator, as it has been explained by Yang and Song (2014), as implemented in LabVIEW. In the end, the averaged damping coefficient was calculated based on the decremental logarithm method over 50 successive oscillatory points of the signal within the envelope. As the damping coefficient of the aluminium specimens is relatively low compared to that of the 3D-FML specimens, a cut-off value of a 3-second time period was applied to aluminium specimens signals while a 0.1-second long signal duration was used for 3D-FML specimens as the time period through which the decremental logarithm (hence, the damping coefficient) were calculated.

3 RESULTS AND DISCUSSION

The results of the experiments and analyses are presented in this section. It is worth mentioning that at least nine tests were conducted per each specimen, and the results are the average of at least 27 tests and analyses for at least three specimens per category. External noise was minimized during impulse excitation. Tappings were applied on the same location between the two supports, close to the center span of each specimen. Tapping on a different location could cause excitation of a different vibration mode and frequency. All the averaged fundamental frequency values of each category obtained experimentally through the use of the LDV, and are shown in Figure 3(a). This chart indicates that the inclusion of 1 wt% MWCNT in the core and/or interface of the 3D-FMLs resulted in a marginal increase of 1.01 times (1.18%) (when only the interface was NP reinforced: 3DFML6) and 1.06 times (6.61%) in the fundamental frequency (when both core and interface were NP reinforced: 3DFML8). On the other hand, average improvements of 3.46 times (246.2%) and 3.49 times (249.1%) in specimen damping ratios were obtained for the two reinforcement scenarios, respectively (see Figure 3(b)). It can also be observed from Figure 3(a) that the theoretical values of the fundamental frequencies are in good agreement with the experimental ones.

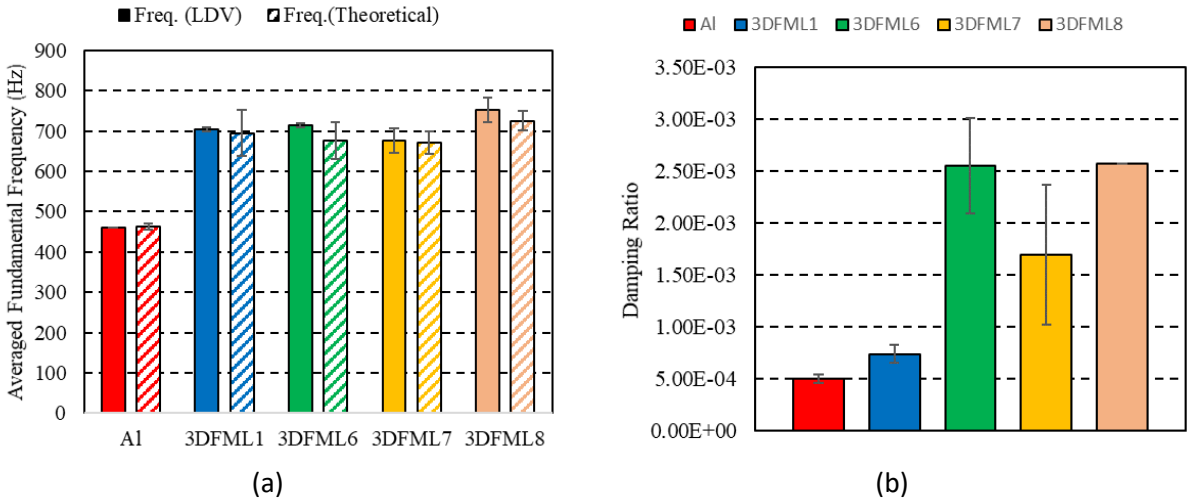

Figure 3: Averaged fundamental frequencies and damping ratios of specimens with free-free boundary conditions

Moreover, the fundamental frequency and damping ratio of specimen type 3DFML7 (only the core was nano-reinforced) were diminished due to defects and NP agglomerations, which were observed as shown in Figure 4 (a). On the other hand, in situations where NPs were uniformly dispersed within the resin, see Figure 4 (b), the increase in frequency and damping ratio (i.e., 3DFML8) is hypothetically associated with the gain in bending rigidity and stiffening of the core (matrix) as a result of NP inclusion. In general, the data indicate that MWCNT reinforcement of 3D-FMLs augments the fundamental frequency marginally, while the damping characteristics of 3D-FMLs were improved quite significantly.

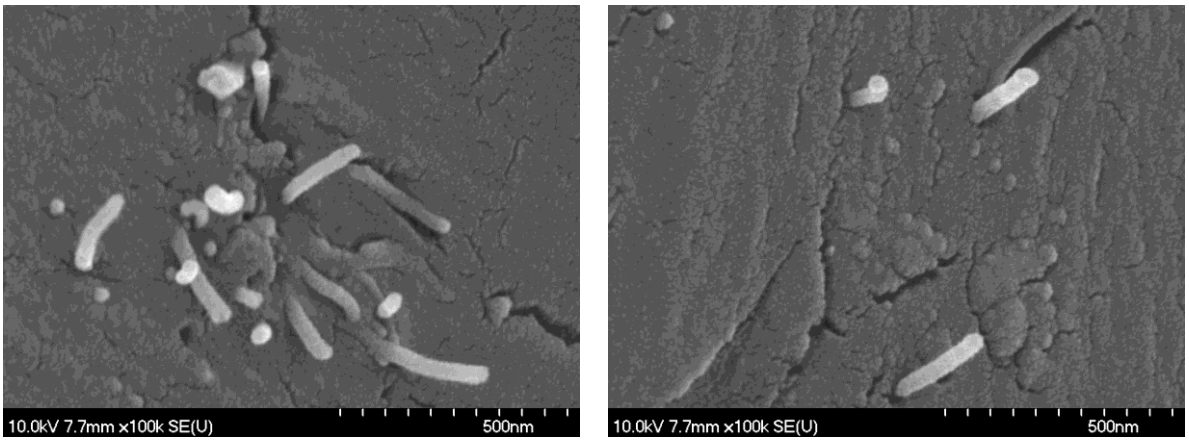

(a) (b)

Figure 4: SEM images of (a) 3DFML7 with anomalous behaviour due to defects and agglomerations of NPs; (b) 3DFML8 with augmented properties due to a uniformity of NP dispersion

4 CONCLUSIONS

The presented research study explored the frequency response of 3D-fiber metal laminates and the effect of nanoparticle modification of the resin matrix. In general, the inclusion of MWCNT in the resin of 3D-fiber metal laminates enhanced the fundamental frequency only marginally but improved the damping response quite significantly.

5 ACKNOWLEDGEMENTS

The authors would like to gratefully acknowledge financial support by the Natural Sciences and Engineering Research Council of Canada and the Sadler Scholarship at the Department of Mechanical Engineering at the University of Alberta.

REFERENCES

Ahmadi-Moghadam, B. *et al.* (2015) 'Effect of functionalization of graphene nanoplatelets on the mechanical response of graphene/epoxy composites', *Materials & Design (1980-2015)*, 66, pp. 142–149.

Ahmadi-Moghadam, B., *et al.* (2013) 'Interlaminar crack detection in graphene nanoplatelet/CFRP composites using electric resistance change', in Suong Van Hoa, P. H. (ed.) *THE 19 TH INTERNATIONAL CONFERENCE ON COMPOSITE MATERIALS*. Montreal: Curran Associates, Inc., pp. 3597–3607.

Asaee, Z. and Taheri, F. (2016) 'Experimental and numerical investigation into the influence of stacking sequence on the low-velocity impact response of new 3D FMLs', *Composite Structures*, 140, pp. 136–146.

Asundi, A. and Choi, A. Y. N. (1997) 'Fiber Metal Laminates: An Advanced Material for Future Aircraft', *Journal of Materials Processing Technology*, 63, pp. 384–394.

Berthelot, J.-M. (1999) *Composite Materials : Mechanical Behavior and Structural Analysis*, *Springer*. Springer.

Berthelot, J.-M. (2005) 'Damping Analysis of Orthotropic Composites with Interleaved Viscoelastic Layers: Modeling'.

Cheraghi, N., *et al.* (2007) 'Application of Hilbert-Huang transform for evaluation of vibration characteristics of plastic pipes using piezoelectric sensors', *Structural Engineering and Mechanics*.

Techno-Press, 25(6), pp. 653–674.

De Cicco, D. and Taheri, F. (2018a) 'Robust numerical approaches for simulating the buckling response of 3D fiber-metal laminates under axial impact-Validation with experimental results'.

De Cicco, D. and Taheri, F. (2018b) 'Use of a Simple Non-Destructive Technique for Evaluation of the Elastic and Vibration Properties of Fiber-Reinforced and 3D Fiber-Metal Laminate Composites', *Fibers*. Multidisciplinary Digital Publishing Institute, 6(1), p. 14.

Devalve, C. and Pitchumani, R. (2013) 'Experimental investigation of the damping enhancement in fiber-reinforced composites with carbon nanotubes'.

Hajikhani, M. *et al.* (2009) 'Monitoring of delamination in composites by use of Acoustic Emission', in *3rd Condition Monitoring & Fault Diagnosis Conference*.

Hyer, M. W. (2009) *Stress Analysis of Fibre-Reinforced Composite Materials*, *DEStech Publications, Inc*.

Kelly, S. G. (1992) *Fundamentals of Mechanical Vibrations*. 2nd edn. New York: McGraw-Hill Education.

Khan, S. U. *et al.* (2011) 'Vibration damping characteristics of carbon fiber-reinforced composites containing multi-walled carbon nanotubes', *Composites Science and Technology*, 71, pp. 1486–1494.

Lei, Z. X., *et al.* (2015) 'Free vibration analysis of laminated FG-CNT reinforced composite rectangular plates using the kp-Ritz method', *Composite Structures*, 127, pp. 245–259.

Liu, A., *et al.* (2011) 'Effect of functionalization of single-wall carbon nanotubes (SWNTs) on the damping characteristics of SWNT-based epoxy composites via multiscale analysis'.

Noor, A. K. (1973) 'Free vibrations of multilayered composite plates.', *AIAA Journal*, 11(7), pp. 1038–1039.

Reddy, J. N. (2004) *Mechanics of Laminated Composite Plates and Shells*. CRC Press.

Sayyad, A. S. and Ghugal, Y. M. (2015) 'On the free vibration analysis of laminated composite and sandwich plates: A review of recent literature with some numerical results', *Composite Structures*. Elsevier, 129, pp. 177–201.

Soltannia, B. *et al.* (2016) 'Parametric Study of Strain Rate Effects on Nanoparticle-Reinforced Polymer Composites'.

Soltannia, B., *et al.* (2013) 'Influence of tensile impact and strain rate on the response of adhesively bonded single lap joints', in Suong Van Hoa, P. H. (ed.) *THE 19TH INTERNATIONAL CONFERENCE ON COMPOSITE MATERIALS*. Montreal: Curran Associates, Inc., pp. 1410–1417.

Soltannia, B. and Taheri, F. (2013) 'Static, Quasi-Static and High Loading Rate Effects on Graphene Nano-Reinforced Adhesively Bonded Single-Lap Joints', *International Journal of Composite Materials*, 3(6), pp. 181–190.

Soltannia, B. and Taheri, F. (2014) 'Influence of nano-reinforcement on the mechanical behavior of adhesively bonded single-lap joints subjected to static, quasi-static, and impact loading'.

Taheri, F. (2017) 'Applications of nanoparticles in adhesives: Current status', in Pizzi, A. and Mittal, K. L. (eds) *Handbook of Adhesive Technology*. Third Edit. Boca Raton, FL: CRC Press, pp. 95–141.

Tedesco, J. W., *et al.* (1999) *STRUCTURAL DYNAMICS: THEORY AND APPLICATION*. Menlo Park, CA: Addison Wesley Longman.

Yang, X., *et al.* (2014) 'Signal Analysis and Processing Platform Based on LabVIEW', *Sensors & Transducers*, 172(6), pp. 165–171.

Zou, G. P., *et al.* (2003) 'A nondestructive method for evaluating natural frequency of glued-laminated beams reinforced with GRP', *Nondestructive Testing and Evaluation*, 19(1), pp. 53–65.